

Novel QR-incorporated chipless RFID tag

Humayun Shahid^{1a)}, Muhammad Ali Riaz¹, Yasar Amin^{1,2},
Adeel Akram¹, Jonathan Loo³, and Hannu Tenhunen^{2,4}

¹ ACTSENA, Department of Telecommunication Engineering, University of Engineering and Technology, Taxila-47050, Punjab, Pakistan

² iPack VINN Excellence Center, Royal Institute of Technology (KTH), Isaffjordsgatn 39, Stockholm, SE-16440, Sweden

³ Department of Computer and Communications Engineering, Middlesex University, UK

⁴ TUCS, Department of Information Technology, University of Turku, Turku-20520, Finland

a) humayun.shahid@uettaxila.edu.pk

Abstract: This work ideates a novel approach for designing a QR-incorporated data encoding structure that functions as a fully-passive, chipless radio frequency identification (RFID) tag. Several concentric square-shaped resonant slots embedded strategically within a QR-patterned region constitute the tag. A functional prototype is realized over an ungrounded Duroid[®] 5880 substrate, and the same is evaluated for its electromagnetic performance. The tag performs encoding of up to 118 data bits distributed across spectral and optical domain in a compact form factor measuring $55 \times 55 \text{ mm}^2$. Possible applications of the formulated tag include multi-layer authentication for secure access control in smart cities and connected homes.

Keywords: chipless RFID, radar cross section, data encoding circuit

Classification: Microwave and millimeter-wave devices, circuits, and modules

References

- [1] S. Preradovic, *et al.*: “Chipless RFID: Bar code of the future,” *IEEE Microw. Mag.* **11** (2010) 87 (DOI: [10.1109/MMM.2010.938571](https://doi.org/10.1109/MMM.2010.938571)).
- [2] M. W. Gallagher, *et al.*: “Mixed orthogonal frequency coded SAW RFID tags,” *IEEE Trans. Ultrason. Ferroelectr. Freq. Control* **60** (2013) 596 (DOI: [10.1109/TUFFC.2013.2601](https://doi.org/10.1109/TUFFC.2013.2601)).
- [3] S. Rauf, *et al.*: “Triangular loop resonator based compact chipless RFID tag,” *IEICE Electron. Express* **14** (2017) 20161262 (DOI: [10.1587/elex.14.20161262](https://doi.org/10.1587/elex.14.20161262)).
- [4] M. A. Riaz, *et al.*: “Novel T-shaped resonator based chipless RFID tag,” *IEICE Electron. Express* **14** (2017) 20170728 (DOI: [10.1587/elex.14.20170728](https://doi.org/10.1587/elex.14.20170728)).
- [5] M. S. Iqbal, *et al.*: “FSS inspired polarization insensitive chipless RFID tag,” *IEICE Electron. Express* **14** (2017) 20170243 (DOI: [10.1587/elex.14.20170243](https://doi.org/10.1587/elex.14.20170243)).
- [6] A. M. Numan-Al-Mobin, *et al.*: “RFID integrated QR code tag antenna,” *IEEE MTT-S International Microwave Symposium* (2015) 1 (DOI: [10.1109/IMWS.2015.7400001](https://doi.org/10.1109/IMWS.2015.7400001)).

- MWSYM.2015.7167044).
- [7] G. S. Vardhan, *et al.*: “QR-code based chipless RFID system for unique identification,” IEEE International Conference on RFID Technology and Applications (RFID-TA) (2016) 35 (DOI: [10.1109/RFID-TA.2016.7750744](https://doi.org/10.1109/RFID-TA.2016.7750744)).
 - [8] D. Betancourt, *et al.*: “Design of printed chipless-RFID tags with QR-code appearance based on genetic algorithm,” IEEE Trans. Antennas Propag. **65** (2017) 2190 (DOI: [10.1109/TAP.2017.2684193](https://doi.org/10.1109/TAP.2017.2684193)).
 - [9] K. Bu, *et al.*: “You can clone but you cannot hide: A survey of clone prevention and detection for RFID,” IEEE Commun. Surveys Tuts. **19** (2017) 1682 (DOI: [10.1109/COMST.2017.2688411](https://doi.org/10.1109/COMST.2017.2688411)).
 - [10] A. Vena, *et al.*: “Chipless RFID tag using hybrid coding technique,” IEEE Trans. Microw. Theory Techn. **59** (2011) 3356 (DOI: [10.1109/TMTT.2011.2171001](https://doi.org/10.1109/TMTT.2011.2171001)).
-

1 Introduction

Optical barcodes, though still in use, are losing ground to quick response (QR) codes and RFID tags [1]. A quick response (QR) code is a machine-readable two-dimensional binary image composed of square patches positioned sequentially on a grid. Information encoded optically in a QR code is readily decodable by low-cost imaging devices such as cellphone cameras. Chipless variants of radio frequency identification (RFID) tags have received considerable research interest in recent past [2, 3, 4, 5]. Both time domain [2] and frequency domain-based chipless RFID tags have been designed, with the latter encoding data in spectral domain and offering advantages such as ease of manufacturing, polarization insensitivity and design compactness [3, 4, 5]. QR codes and RFID tags, when unified, can act as an effective security contraption offering multi-layer authentication. The resulting artifact holds potential for enhanced access control and reduced counterfeiting events. QR-integrated chip-based RFID tag reported in literature remains expensive for mass deployment in low-end applications due to dedicated silicon chip [6]. A retransmission-based chipless RFID tag based on QR-patterned resonators has been demonstrated [7]. The tag, however, requires antennas for operation in full-wireless mode. A novel approach for designing chipless RFID tags based on genetic algorithms is proposed, where the resulting RFID tags do have a QR-code appearance yet contain no optical-encoded information [8]. This work ideates a full-wireless, QR-code incorporated, chipless RFID tag. Error correction features of QR-code are leveraged to store information in both spectral and optical domains. The proposed design allows for encoding of up to 08 data bits in the spectral domain as well as up to 110 bits (i.e. 20 alphanumeric characters) in the optical domain. The formulated tag, realized over compact physical dimensions of $5.5\text{ cm} \times 5.5\text{ cm}$, offers an information density of 3.90 bits/cm^2 . Possible use includes counterfeit-deterrent tags for access control, smart ticketing, intelligent packaging and similar applications.

2 Unification strategy

Chip-based RFID tags remain prone to cloning, compromising their suitability for

impeccably secure access control [9]. A possible solution is to use chipless RFID tags, whereby access key cloning becomes challenging. The proposed approach distributes encoding of the access key across both optical and spectral domains. Consequently, cloning is deterred by rendering the process significantly difficult and time-consuming. Generally, QR-codes are equipped with error-correction features that allow for decoding of data even when the QR-patterned region is obscured or defaced. Out of the four standard error correction levels, the most commonly used one is level-M, allowing a QR-code to sustain as much as 15% damage to its real estate.

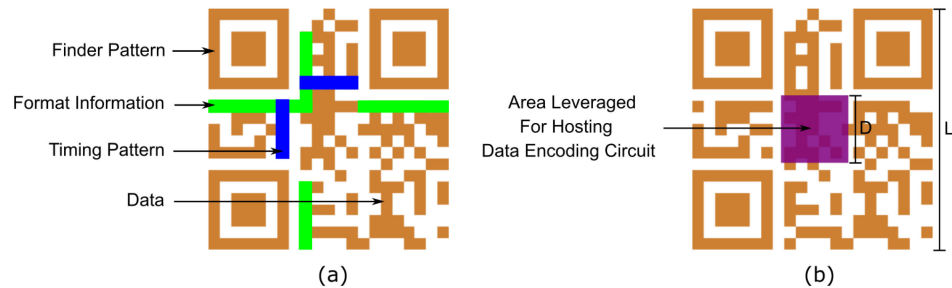


Fig. 1. (a) Anatomy of a typical level-M QR-code.
(b) Area for hosting data encoding circuit.

Anatomy of a typical level-M fortified QR-code encoding alphanumeric characters is depicted in Fig. 1(a). Various portions such as the finder pattern, timing pattern, format information (including error correction version) and the encoded data itself are demarcated. Fig. 1(b) highlights the resulting 15% area (excluding the finder patterns) altering which does not affect the readability of the optical-encoded data. The novel unification strategy is essentially based on leveraging this highlighted area in the middle of the QR-code to host an electromagnetic data encoding circuit, successfully unifying QR-code and chipless RFID technology.

3 Working principle and encoding circuit design

In order to ensure that the proposed tag is not bulky and fits conveniently into a wallet or purse, L is chosen to be 55 mm. This choice of geometrical parameters is in line with the standard credit card dimensions. Given that L equals 55 mm and level-M error correction is in place, D is calculated to be 15.5 mm. The specifications necessitate design of an electromagnetic resonant circuit that readily fits a $15.5 \times 15.5 \text{ mm}^2$ square-shaped region in the middle of the QR-code, and encodes an arbitrary bit sequence in the spectral domain. Inspiration is drawn from recent work on multi-resonant chipless RFID tags [3, 4, 5]. The resonant circuits reported therein are composed of several resonant elements patterned in a concentric fashion on appropriately-sized grounded substrate. As evident in Fig. 1(b), L is greater than D , implying that for the encoding circuit to be designed, the substrate will extend beyond the geometrical bounds of the resonant elements. With the above constraint in place, the optimal choice is to use negatively etched resonant slots for realizing the encoding circuit. For a single square-shaped resonant slot depicted in Fig. 2(a), distribution of surface current that takes effect when a horizontally polarized wave

at 8.0 GHz impinges upon the structure is shown in Fig. 2(b). It is evident that the surface current is concentrated maximally towards the exterior of the square-shaped slot, signifying inductive effects. On the other hand, the same tends to be minimum towards the inner periphery of the resonant slot, indicating capacitive characteristics. This peculiar coexistence of inductive and capacitive components along a single square-shaped slot generates a resonance at specific frequency value. The resonance manifests as a readily identifiable dip in the RCS response, as shown in Fig. 2(c).

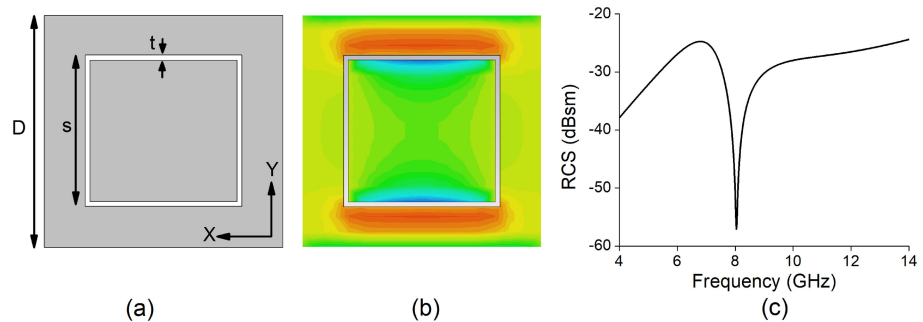


Fig. 2. (a) Single slot with $s = 10$ mm and $t = 0.3$ mm.
(b) Surface current density at 8.0 GHz.
(c) RCS response of resonant slot.

A loop-based design strategy is followed for designing the electromagnetic data encoding circuit. A series of square-shaped slots are patterned in a concentric fashion over an ungrounded 0.13 mm thick RT Duroid® 5880 substrate. The peculiar structural nesting allowing for attainment of multi-resonant behavior.

Table I. Optimum dimensions of slots.

	s_1	s_2	s_3	s_4	s_5	s_6	s_7	s_8
Slot length (mm)	14.8	13.6	12.4	11.2	10	8.8	7.6	6.4

Precise values of the geometrical parameters for an 8-bit electromagnetic data encoding circuit, optimized iteratively using CST® Microwave Studio® (CST® MWS®), are tabulated in Table I. Note that s_1 represents dimensions of the outermost slot whereas s_8 signifies the same for the innermost one. All resonant slots have the same slot-width, t , and also exhibit a consistent inter-slot spacing, g . Moreover, both t and g measure the same, and are equal to 0.3 mm. The design also entails de-metalization of the substrate beyond the outer-most resonant slot. This accentuates the spectral response of the resonant slots while liberating ample estate for hosting the QR pattern.

The tag prototype, placed next to a standard debit card for size comparison purpose, is presented in Fig. 3(a). The prototype offers highly sought-after features of compactness and portability. The QR-incorporated is presented in Fig. 3(b), where the QR-patterned portion is realized on paper using non-conductive color-matched ink. By configuring the QR-pattern and data encoding circuit on the same side of the substrate, vacant portion at the back can be modified as per constraints associated with various applications and challenging environments. For instance, a layer of silicon can be provisioned on the back, mitigating the effects of coupling in



Fig. 3. (a) Electromagnetic data encoding circuit.
(b) QR-incorporated chipless tag.

body-centric applications. The back can also undergo appropriate metalization to support on-metal deployment. Mid-frontal cut-out eliminates contact between resonators and paper, ensuring insensitivity to moderate humidity changes.

4 Results and discussion

Electromagnetic performance descriptors for the proposed data encoding circuit are discussed. All computer-aided simulations that appear in this section are performed using CST[®] MWS[®]. The proposed QR-unified tag is also evaluated for its electromagnetic performance. The arrangement for making experimental observations follows [10], involves two identical linearly-polarized antennae, vector network analyzer (VNA) R&S[®] ZVB-20 and multiple tag prototypes. Testing is performed in non-anechoic laboratory environment ($T = 23 \pm 5^\circ\text{C}$, $\text{RH} \leq 45\%$). Tag under test is affixed on a 90 mm thick block of closed-cell rigid foam 51 HF from ROHACELL[®]. Consider distributed encoding of a 21 character alphanumeric passkey, where the most significant byte is an 8-bit long ASCII character encoded in the spectral domain, as shown in Fig. 4, and remaining alphanumeric characters are encoded in the optical domain using QR code version 01 and error correction level-M.

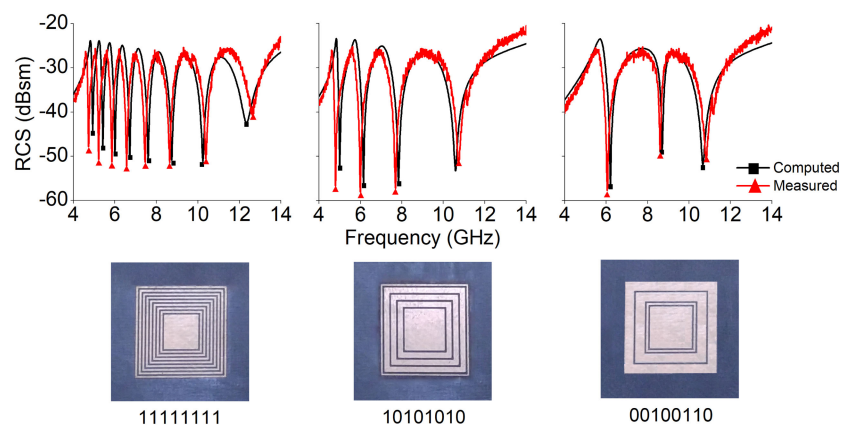


Fig. 4. Spectral encoding of all-1s, alternating and randomized bit sequence.

The simulated performance and the experimental measurement exhibit good overall agreement. Though a slight drift is observable in a few resonant dips, the encoded data remains intelligible. The drift is due to imperfections in the prototype realization process. Since the structure is not backed by a ground plane, placing the

tag on conductive surfaces deteriorates the RCS response. On the other hand, the proposed tag does retain its electromagnetic performance when placed on dielectric materials such as closed-cell foam.

Table II. Comparison with other shaped resonators.

Work	Bits encoded (Spectral Domain)	Bits encoded (Optical Domain)	Physical Dimensions	Cumulative Bit Density (bits/cm ²)
Betancourt <i>et al.</i> [8]	08	zero	3 × 3 cm ²	0.9
Vardhan <i>et al.</i> [7]	03	115	20 × 5.5 cm ²	1.07
Proposed design	08	110	5.5 × 5.5 cm ²	3.9

Table II compares the proposed approach with previously reported work. Owing to a compact form factor, the bit density offered by the proposed design stands convincingly higher.

5 Conclusion

A QR-incorporated chipless RFID tag designed using a novel unification strategy is proposed. The tag encodes up to 118 data bits, is realized over compact dimensions of 5.5 × 5.5 cm². The formulated tag offers enhanced bit density as well as multi-layer authentication in a minuscule form factor. Proposed tag offers secure access control in smart cities and connected homes.

Acknowledgments

UET, Taxila is thanked for ACTSENA research fund. NIE, Islamabad, also.